

CFA '18 LE HAVRE ■ 23-27 avril 2018
14^{ème} Congrès Français d'Acoustique



Modeling for Wave Propagation and Energy Losses in Solids with Cracks: the MMD-FEM Code

V. Aleshin^a, S. Delrue^b et K. Truyaert^b

^aIEMN CNRS UMR8520, Cité Scientifique Avenue Henri Poincaré CS 60069, 59652 Villeneuve D'Ascq, France

^bKU Leuven, KU Leuven Kulak, E. Sabbelaan 53, 8500 Kortrijk, Belgique
aleshin@mail.ru

The importance of modeling in NDT is due to the fact that it allows one to interpret experimentally measured indicators and finally retrieve parameters of damage. This concern stimulated us to develop modeling support for nonlinear ultrasound techniques by combining commercially available finite element software with a realistic contact model based on the original Method of Memory Diagrams (MMD). The method has been recently proposed for automating the account for friction-induced hysteresis in the mechanical response of rough surfaces excited by arbitrarily changing normal and tangential displacements. The resulting load-displacement relationship represents a boundary condition that has to be set at surfaces of inner boundaries appearing in a material with cracks. The boundary condition is then used by the FEM code for calculation of stresses and strains in the material's volume. In practice, the FEM part has been programmed in COMSOL that enables a relatively simple implementation of user-defined boundary conditions calculated in an external MATLAB procedure. The advantage of the MMD-FEM modeling toolbox is in its computational efficiency that results from the multiscale approach in which the influence of microscopic features (roughness) is integrated in the response of a mesoscopic cell (crack segment), drastically simplifying the account for rough contact geometry. Moreover, the instantaneous friction-induced loss of mechanical energy is also easily calculated making it possible to add the heat transport module and to study heat diffusion in materials with acoustically excited cracks. We give some calculation examples and show how the suggested toolbox assists nonlinear NDT methods. Examples concerning the ultrasound propagation and nonlinear acoustic effects are also considered.

1 Introduction

The proposed study is at the interface between nonlinear acoustics and contact mechanics. It uses a contact mechanical model to calculate load-displacement relationships for frictional contacts. As a result, a multitude of wave and vibration problems for materials containing such frictional contacts can be numerically solved. The contact model used here is based on certain compromises related to the level of complexity and realism.

On one hand, the modeling of internal contacts is possible using elementary models in which a simple (frequently linear) load-displacement relation is postulated. An example is the diode-type model that uses different elastic moduli for normal compression and tension. However, elementary models are unable to represent one of the major mechanisms responsible for nonlinear behavior of materials: friction at internal contacts. Introducing friction into the models drastically increases the complexity level and makes the system hysteretic and memory-dependent.

On the other hand, the modeling of frictional contact responses is possible by using purely numerical approaches of contact mechanics [1]. Doing so, all particular interaction laws and movement types can be taken into account. The difficulty related to this approach is in the implicit character of the procedure. Indeed, accepting the Coulomb friction law for representing interactions of flat contact faces [2] does not provide an explicit link between contact loads and displacements. To obtain that link, an iterative procedure is necessary which assumes some trial contact face displacements and then tries to adjust them to satisfy the Coulomb conditions. Such methods are intensively developed [2] despite high computational expenses arising due to implicit calculations of complex hysteretic dependencies.

The compromise we propose is based on a semi-analytical model in contact mechanics that can also be referred to as a generalized Hertz-Mindlin approach. The classical Hertz-Mindlin solution [3] is the load-displacement relationship for a tangential shift of two spheres with friction, excited by a number of specific loading protocols, such as constant oblique loading, oblique loading-unloading-reloading series, oscillatory oblique loading, etc. Here the solution is extended to the case of non-spherical geometries including rough surfaces. This means that the contact surfaces are represented as a

collection of fragments (or mesoscopic cells) in which loads and displacements are considered as mean values (not fields), as shown in Figure 1. Moreover, the account for various loading histories is automated by establishing general rules that allow one to link loads and displacements via a universal integral representation derived from the Coulomb friction law.

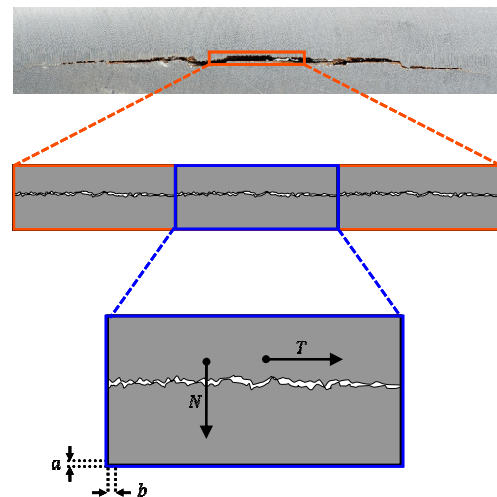


Figure 1: Contact problem at the mesoscopic scale: a link between loads (contact forces per unit nominal contact surface) N and T , and displacements a and b should be determined.

The account for surface roughness is essential for the proposed model. Rough surfaces recede under both normal and tangential loading because of deformation of asperities. Therefore, contact displacements can be determined in the framework of the contact model itself and not by external conditions. For instance, the tangential displacement between two perfectly flat surfaces with friction is not defined by the Coulomb friction law, but by the influence of surrounding material. In our approach, this difficulty is avoided for the price of complication of the contact model, but the contact model and the elasticity equations in the bulk material become uncoupled.

The approach is discussed in the next sections in more detail. Here a two-dimensional model is presented.

2 Method of memory diagrams for partial slip

Frictional mechanical contact between two profiles can be found in one of three states depending on loading conditions: no contact, total sliding, and partial slip. The latter situation occurs due to the presence of surface relief, since surface points having different heights are compressed differently, and the normal and shear stresses determining stick and slip are different at different points. We will consider this particular situation first, and will then extend the established solutions to the other two (more trivial) cases.

The link between loads N and T , and displacements a and b (see Figure 1) is established by application of the Method of Memory Diagrams (MMD) in which an internal memory function (or memory diagram) responsible for all hysteretic effects is introduced. The MMD is based, in turn, on the Reduced Elastic Friction Principle (REFP, [4,5]) which states that for a frictional system (axisymmetric or with rough faces), the tangential loads and displacements can be expressed through the normal ones in the following way:

$$\begin{cases} b = \theta\mu(a - q) \\ T = \mu \left(N(a) - N(a) \Big|_{a=q} \right) \end{cases}, \quad (1)$$

where the normal load-displacement relationship $N=N(a)$ is considered to be known, μ is the friction coefficient, q is a displacement-related parameter that has to be calculated for known a and b , and θ is a material constant that depends only on Poisson's ratio ν ,

$$\theta = \frac{2 - \nu}{2(1 - \nu)}. \quad (2)$$

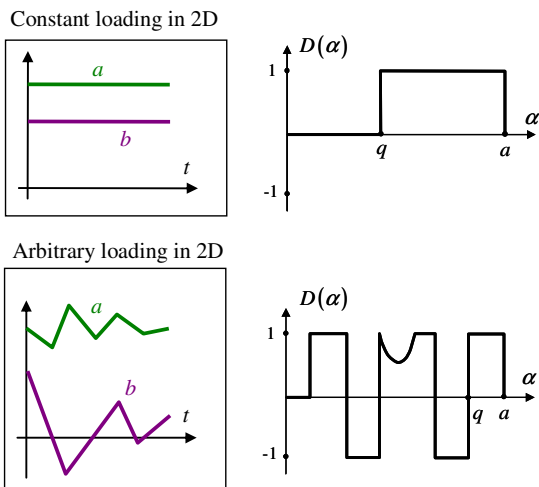


Figure 2: Loading histories (constant and arbitrary loading) and corresponding memory diagrams.

Eq. 1 can be rewritten in the following form:

$$\begin{cases} b = \theta\mu \int_0^a D(\alpha) d\alpha \\ T = \mu \int_0^a D(\alpha) \frac{dN}{da} \Big|_{a=\alpha} d\alpha \end{cases}, \quad (3)$$

in which $D(\alpha)$ is the memory diagram function which for constant loading is defined as in Figure 2 (upper right corner). Using the MMD, it is possible to show that Eq. (3) also holds in the case of arbitrary loading in 2D, whereas the memory diagram $D(\alpha)$ becomes more complex (Figure 2, lower line).

In [6], a set of rules are established which allow one to update the memory diagram following the evolution of a drive parameter (here displacement b) and then calculate the output (here tangential load T) thus constructing the sought-for load-displacement relationship.

In fact, the solution in the arbitrary excitation case is represented as a superposition of the basic solutions Eq. (1), with numerous parameters being "memorized" during the evolution. The memory diagram represents a way of keeping track of these parameters. Its interpretation is especially simple in the constant-loading case Eq. (1). Here, slip is induced by application of a constant tangential displacement b while keeping constant normal displacement a . The slip zone is determined by parameter q . Slip progresses in such a way that the remaining stick zone coincides with the contact zone that would be created by application of the reduced normal displacement $a=q$ (see Figure 3). The corresponding memory diagram has a constant section $q < \alpha < a$ which indicates the presence of the corresponding slip process.

The more complicated memory diagram in Figure 2 basically represents a similar thing except that both a and b can vary. In [6] it is demonstrated that curvilinear sections in the memory diagram are created during the process when the normal compression enlarges the contact spots so rapidly that it "overruns" the slip propagation that always departs from the contact periphery and progresses towards the contact center. In this case, slip does not occur and $q=a$.

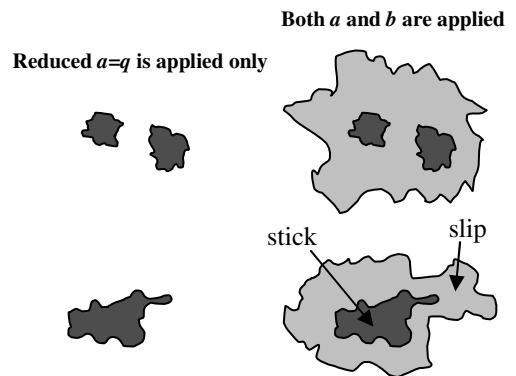


Figure 3: Loading histories (constant and arbitrary loading) and corresponding memory diagrams.

The MMD is applicable when the load-displacement relationship $N=N(a)$ is known. In our example we use a quadratic normal reaction curve $N(a) \sim a^2$ as suggested in [7] on the basis of experimental and theoretical arguments.

The MMD can be formulated for both displacement-driven and force-driven systems, with a formal representation $T=MMD(b)$ or $b=MMD(t)$. However, as it is shown in the next section, the extension to the total sliding case is particularly simple for the displacement-driven system.

3 Total sliding and no contact cases

When $|T|$ reached μN i.e. $|b|$ reaches $\theta\mu a$, the total sliding process in which the stick zone completely disappears is about to start. If T is considered as an input in the contact model, b becomes undetermined in this case and depends on stress or strain fields in the surrounding material. This is something to be avoided since for explicit calculations the boundary condition should be posed independently of the surrounding stresses and strains. If not, the use of the MMD does not present any benefit. A way of avoiding this difficulty is setting b as an input parameter and considering T is an output parameter. To account for full sliding, b can be represented as a sum of two components [8]:

$$b = b_0 + \tilde{b}. \quad (4)$$

where b_0 corresponds to the displacement achieved in the total sliding regime (i.e. the mismatch between two closest points belonging to the opposite faces experiencing the highest normal stress in compression), and \tilde{b} is a component that reflects partial slip and the ability of asperities to recede under tangential load. Eq. (4) allows one to write down the solutions for each contact regime: no contact, partial slip, and total sliding.

- Contact disappears when $a \leq 0$. Since no contact interaction is present, $N=T=0$, and asperities remain unstrained, i.e. $\tilde{b} = 0$. Correspondingly, $b_0 = b$ in this case. The memory function equals 0 everywhere for $0 \leq \alpha \leq a$ (Figure 4(a)).
- Partial slip takes place when $a > 0$, $|\tilde{b}| < \theta\mu a$. In accordance to the MMD applicable in this situation, $T = MMD(\tilde{b})$ while the total sliding contribution b_0 remains unchanged. The memory diagram has a certain form depending on loading history (Figure 4(b)).
- Total sliding happens when $a > 0$ and the memory function equals +1 or -1 on the whole interval $0 \leq \alpha \leq a$ (Figure 4(c)). According to Eq. (1), $\tilde{b} = \pm\theta\mu a$ where the sign depends on the direction of sliding. The asperities recede under tangential loading, so that the actual full sliding contribution should account for this effect: $b_0 = b - \tilde{b}$.

So, in summary, there are simple criterions for distinguishing the contact regimes, and in each case either the partial slip component \tilde{b} , either the total sliding contribution b_0 is known, therefore the remaining component is known too, since their sum is a known input parameter.

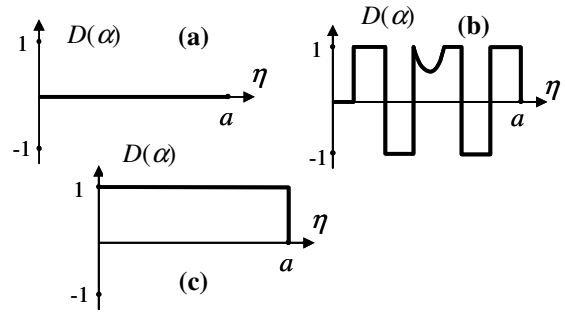


Figure 4: Memory diagrams in three contact regimes: (a) no contact, (b) partial slip, (c) total sliding.

The repartition Eq. (4) completes the contact model based on MMD. Figure 5 illustrates an example of the tangential load-displacement curve (b) calculated for displacements histories (a) containing a dozen of oscillations for imitating a fragment of a typical acoustic signal. In this example, we introduce a characteristic value a_0 of the normal displacement and use the following normalizations: a on a_0 , b on $\theta\mu a_0$, N on $N(a_0)$, T on $\mu N(a_0)$.

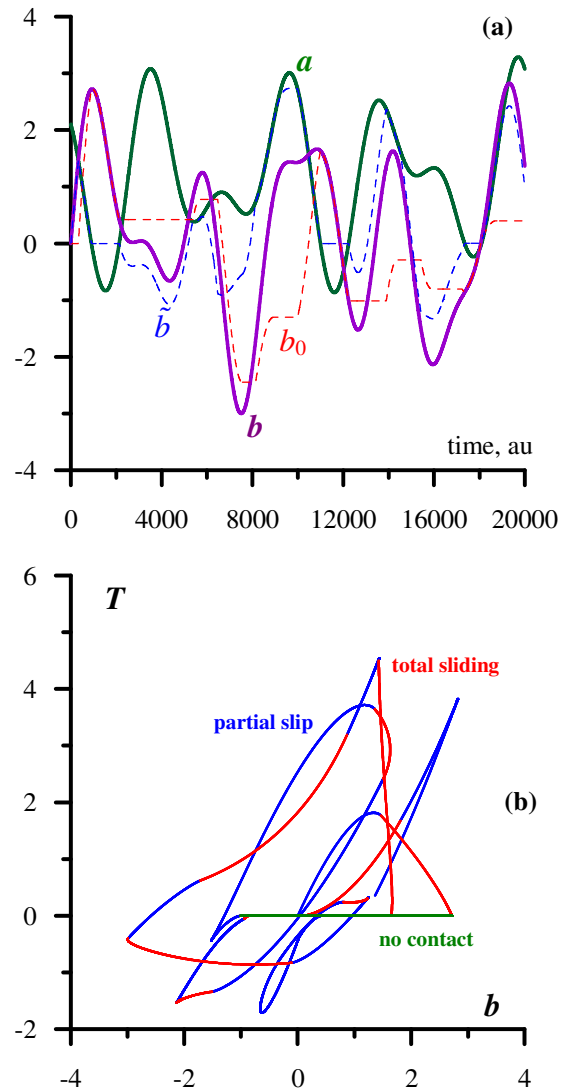


Figure 5: Tangential load-displacement relationship (b) calculated using our contact model for an exemplar displacements history (a).

4 Friction-induced energy loss

The MMD also allows one to calculate friction-induced energy loss, i.e. the work done by friction forces in a contact system. Strictly speaking, this can be done for an axisymmetric system in which stress and displacement fields are given by known particular expressions. For a pair of rough surfaces in contact, these fields are not known and are very complex. However, if two mechanical systems have the same dynamic behavior they also have the same energetic behavior, which means that they dissipate the same amount of energy. The existence of an equivalent axisymmetric system for a pair of rough surfaces is guaranteed by the REFP (with some assumptions listed in the concluding section).

A detailed analysis will be published elsewhere and results in the following expression for an incremental energy loss occurring when the displacements a and b change by small increments $\Delta a, \Delta b$:

$$\Delta W = 2\mu(|\Delta b| - \theta\mu\Delta a) \left[N(a) - N(q) + \frac{dN}{da} \Big|_{a=q} (q - a) \right] \quad (5)$$

This equation includes the total sliding regime when $q=0$, and $N(a=q=0)=0$. It is possible to show that $dN/da=0$ at $a=q=0$, too. The term $-\theta\mu\Delta a$ is important here. In particular, for total sliding it describes the difference between infinitesimal slip distance contributing to the friction force work, and the bulk displacement increment, Δb . These two values are different since contact of rough surfaces is not absolutely rigid in the tangential direction. In fact, asperities recede under tangential action, and the associated stiffness depends on compression. Figure 6 illustrates the accumulating energy loss for the same excitation history as in Figure 5.

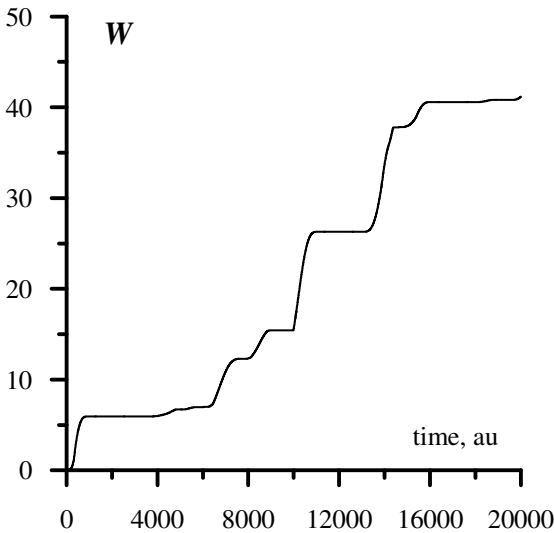


Figure 6: Accumulated friction-induced energy loss corresponding to the incremental loss ΔW in Eq. 5.

The energy loss is normalized on $\theta\mu^2 N(a_0)$. Horizontal parts of the curve correspond to one of two situations: no mechanical contact between surfaces, and the case of "overloading" briefly described in section 3 (before Figure 3). In the latter case, Δa is positive and large enough to reach $\theta\mu\Delta b$. Hence, contact spots enlarge so rapidly that

slip commencing at the contact periphery and propagating inward can not develop.

5 Wave propagation example

The presented contact model has been used as an external boundary condition that is to be set at the boundary corresponding to the internal contact [9]. Such a possibility is offered by the "thin elastic layer" feature available in the solid mechanics module of COMSOL Multiphysics. Figure 7 shows a simulation example for a test sample (aluminum block) with an inclined crack of known geometry (set (a)). The geometry has been automatically meshed with a variable mesh size which drastically decreases in the vicinity of the crack (set (b)). The normal reaction curve was taken from literature [7] on ultrasonic assessment of properties of contact between two aluminum samples. Finally, the two pictures (c) and (d) present snapshots of the simulated wave propagation pattern at two different moments of time.

Nonlinear analysis [9,10] of the wave propagation simulation results provides nonlinear signatures of damage and, finally, an opportunity of using the method for nonlinear nondestructive testing and evaluation. The modeling of temperature effects associated with wave propagation is now in progress.

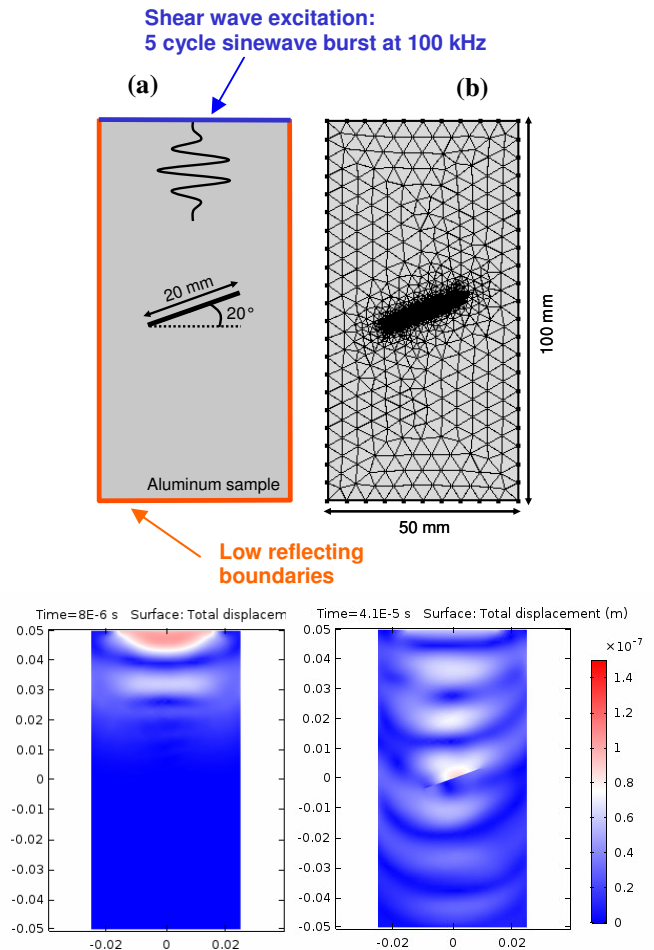


Figure 7: Simulation for a wave propagation in an aluminum sample containing an inclined crack. The considered geometry (original (a) and meshed (b)) is shown as well as two snapshots ((c) and (d)) of the simulated wave propagation pattern.

6 Conclusions

This communication concerns a contact model based on the semi-analytical solutions in contact mechanics provided by the method of memory diagram. The method has a restricted applicability in comparison to purely numerical approaches in contact mechanics but has an enhanced numerical performance suitable for description of acoustic or random signals. The method has the following essential features:

- the considered contact interactions model includes friction and is based on the Coulomb friction law;
- the internal contact/crack surfaces have a nontrivial topography (e.g. roughness);
- Some normal load-displacement curve is postulated (measured or obtained using known modeling approaches);
- the tangential interactions appear during shift; rolling and torsion as movement types are not considered;
- plasticity and adhesion are neglected;
- the model is quasi-static, i.e. frictional dynamics effects are ignored.
- the contact load-displacement solution is obtained via the Method of Memory Diagrams (MMD) [6] that uses the assumptions of the Reduced Elastic Friction principle [4,5].
- In particular, all vectors normal to contact spots are aligned and stay aligned during loading, elastic dissimilarity effects [6 and references therein] are ignored, etc.

The contact model has been integrated into COMSOL finite element software [9] using the possibility to add externally defined boundary conditions calculated in an external MATLAB procedure. The developed numerical tool (MMD-FEM code) can be applied as modeling support for modern nonlinear acoustic NDT methods. Upon the experimental validation, the developed tool is to be used for comparison of data and modeling results and for estimation of geometrical parameters of damage. Its application actually completes an NDT algorithm that starts with nonlinear acoustic measurements and finally results in the estimation of the damage "degree of gravity" and in possible predictions for the lifetime of the sample. In general, numerical modeling considerably increases the visibility and "transparency" of all physical processes used for damage detection.

Acknowledgements

The research leading to these results has gratefully received funding from Internal Funds KU Leuven (C24/15/021) and the European Union Seventh Framework Program (FP7/2007–2013) under Grant Agreement n° 314768 (ALAMSA).

References

- [1] V.A. Yastrebov, *Numerical methods in contact mechanics*, Wiley-ISTE (2013).
- [2] P. Blanloeuil, A. Meziane, C. Bacon, Numerical study of nonlinear interaction between a crack and elastic waves under an oblique incidence, *Wave Motion* **51**, 425–437 (2014).
- [3] R. Mindlin, H. Deresiewicz, Elastic spheres in contact under varying oblique forces, *J. Appl. Mech.* **20**, 327–344 (1953).
- [4] J. Jäger, A New Principle in Contact Mechanics, *J. Tribol.* **120**, 677–684 (1998).
- [5] M. Ciavarella, The generalized Cattaneo partial slip plane contact problem. I - Theory, II - Examples, *Int. J. Solids Struct.* **35**, 2349–2362 (1998).
- [6] V. Aleshin, O. Bou Matar, K. Van Den Abeele, Method of memory diagrams for mechanical frictional contacts subject to arbitrary 2D loading, *Int. J. Sol. Struct.* **60-61**, 84-95 (2015).
- [7] S. Biwa, S. Nakajima, N. Ohno, On the Acoustic nonlinearity of solid-solid contact with pressure-dependent interface stiffness, *Journal of Applied Mechanics* **71**, 508–515 (2004).
- [8] V. Aleshin, S. Delrue, A. Trifonov, O. Bou Matar, K. Van Den Abeele, Two dimensional modeling of elastic wave propagation in solids containing cracks with rough surfaces and friction - Part I: Theoretical background, *Ultrasonics*, **82**, 11-18 (2018)
- [9] S. Delrue, V. Aleshin, K. Truyaert, O. Bou Matar, K. Van Den Abeele, Two dimensional modeling of elastic wave propagation in solids containing cracks with rough surfaces and friction - Part II: Numerical implementation, *Ultrasonics*, **82**, 19-30 (2018).
- [10] S. Delrue, V. Aleshin, M. Sorensen, L. De Lathauwer, Simulation study of the localization of a near-surface crack using an air-coupled ultrasonic sensor array. *Sensors* **17**, art.nr. 930 (2017).